npj | vaccines

Article

Published in partnership with the Sealy Institute for Vaccine Sciences

https://doi.org/10.1038/s41541-025-01336-1

mRNA-lipid nanoparticle vaccines provide protection against lethal Nipah virus infection

Tong Sun[1,6], Yanfeng Yao[2,3,6], Chuanwen Tian[1,4], Yun Peng[3], Yingnan Liu[4], Ge Gao[3], Zhisheng Li[4], Hang Liu[3], Jingyi Han[4], Miaoyu Chen[3], Shuqi Xiao[3], Zhiming Yuan[2,3,5], Chao Shan[2,3,5] ✉, Jingyi Liu[1] ✉ & Hongjun Chen[1,4] ✉

Nipah virus (NiV) is a zoonotic pathogen that causes severe encephalitis and respiratory disease in humans and multiple mammalian species. However, no licensed vaccines or therapeutics are currently available against NiV infection. In this study, we developed three mRNA vaccine candidates using a lipid nanoparticle (LNP) delivery platform: mRNA-F-LNP, comprising mRNA encoding the fusion protein (F); mRNA-G-LNP, containing mRNA encoding the attachment glycoprotein (G); and mRNA-GF-LNP, in which mRNAs encoding both F and G proteins were co-encapsulated at a 1:1 molar ratio. All three mRNA-LNPs induced robust and sustained immune responses in both mice and Syrian hamsters. Sera from immunized Syrian hamster showed high levels of cross-neutralizing antibodies against both NiV-Malaysia (NiV-M) and NiV-Bangladesh (NiV-B) strains. Notably, all three mRNA-LNPs conferred complete protection against a lethal challenge with NiV-M in Syrian hamsters. These findings demonstrate that these mRNA-based vaccines are highly immunogenic and efficacious, highlighting their potential as promising candidates for NiV vaccine development.

Nipah virus disease is a highly virulent zoonotic infection caused by Nipah virus (NiV), which was first identified in 1998 during an outbreak among pig farms in Malaysia[1,2]. Fruit bats of the genus Pteropus are the main natural reservoir of NiV[3]. Human infection can lead to severe disease characterized by encephalitis and respiratory symptoms, with high case fatality rates[4]. Beyond humans, other mammals, including pigs, horses, dogs and cats, are susceptible to NiV infection[5–7]. Since its initial emergence, NiV has caused recurrent outbreaks in several countries across Southeast and South Asia, with a notable outbreak reported in Kerala, India, in 2024 — the sixth in that region since 2018[8]. Two major strains, NiV-Malaysia (NiV-M) and NiV-Bangladesh (NiV-B), have been reported in human outbreaks and are associated with varying clinical severity and mortality rates[9,10]. Due to its high pathogenicity and epidemic potential, NiV is classified as a Risk Group 4 (RG-4) agent and has been designated a priority pathogen by the World Health Organization (WHO)[9].

As a member of the Paramyxoviridae family[11], NiV encodes two essential surface glycoproteins: the attachment glycoprotein (G) and the fusion protein (F). The G protein mediates viral entry through binding to highly conserved ephrin B2/B3 receptors[12], a key step that may explain NiV's broad host range[13,14]. This receptor binding triggers conformational changes in the F protein, leading to its cleavage by host proteases into F1/F2 subunits, enabling membrane fusion and viral entry[15]. Given their essential roles in the viral life cycle, surface accessibility, and strong immunogenicity, both F and G proteins are recognized as key protective antigens and primary targets for neutralizing antibodies and vaccine development[16].

Current strategies for vaccine development against NiV include several platforms: recombinant viral vectors, such as those based on vesicular stomatitis virus (rVSV)[17–20], canarypox virus (rALVAC)[21], vaccinia virus[22], adeno-associated virus[23], and measles virus[24]; subunit vaccines based on the soluble G protein (sG) of NiV and Hendra virus (HeV)[25]; and nucleic acid vaccines and immunoinformatics-designed immunogens. For example, one study developed a structurally stabilized multi-epitope vaccine whose immunogenicity was enhanced by computational prediction of B-cell and T-cell epitopes[26]. While numerous vaccine candidates can induce neutralizing antibodies, only three have progressed to Phase I clinical trials:

[1]Shanghai Veterinary Research Institute, Chinese Academy of Agricultural Sciences, Shanghai, China. [2]State Key Laboratory of Virology and Biosafety, Wuhan Institute of Virology, Chinese Academy of Sciences, Wuhan, China. [3]Center for Biosafety Mega-Science, Wuhan Institute of Virology, Chinese Academy of Sciences, Wuhan, China. [4]State Key Laboratory of Veterinary Public Health and Safety, College of Veterinary Medicine, China Agricultural University, Beijing, China. [5]University of the Chinese Academy of Sciences, Beijing, China. [6]These authors contributed equally: Tong Sun, Yanfeng Yao. ✉e-mail: shanchao@wh.iov.cn; liujingyi@shvri.ac.cn; vetchj@cau.edu.cn

PHV02 (RVSV-Nipah Virus Vaccine Candidate), HeV-sG-V (Hendra Virus Soluble Glycoprotein Vaccine), and mRNA-1215 (NiV mRNA Vaccine)[27].

The mRNA vaccine technology has emerged as a promising platform against emerging pathogens, owing to its distinct advantages such as rapid development timelines, flexible antigen design, robust induction of both humoral and cellular immune response, and an excellent safety profile[28]. In this study, we developed three mRNA-lipid nanoparticle (mRNA-LNP) vaccine candidates: mRNA-F-LNP encoding the F protein, mRNA-G-LNP encoding the G protein, and mRNA-GF-LNP co-expressing both F and G proteins. These candidates were evaluated in both mice and Syrian hamsters. All three vaccines induced durable, high-titer antibodies with neutralizing activity against NiV pseudoviruses and live viruses. Notably, all vaccinated Syrian hamsters demonstrated 100% survival following lethal NiV-M challenge.

Results

Preparation of mRNA vaccines

To develop an effective NiV vaccine, we optimized the codon usage of the full-length F and G glycoprotein genes derived from the NiV-M strain and cloned them into the pcDNA3.1 vector, generating recombinant plasmids pcDNA3.1-F and pcDNA3.1-G. For mRNA production, the plasmids were amplificated by PCR using a downstream primer containing a defined poly(T) sequence to generate the poly(A) tail. The products were subsequently subjected to in vitro transcription and capping, yielding mRNA-F and mRNA-G, respectively (Fig. 1a).

Following purification, the mRNAs were encapsulated into LNP using a standard formulation (SM-102: DSPC: cholesterol: DMG-PEG2000 at 50:10:38.5:1.5 molar ratio), generating three vaccine candidates: mRNA-F-LNP, mRNA-G-LNP, and mRNA-GF-LNP. The mRNA-GF-LNP formulation was generated by co-encapsulating mRNA-F and mRNA-G at a 1:1 molar ratio within the same LNP system. This co-encapsulation approach ensures synchronized delivery of both antigen-encoding mRNAs to target cells, potentially enabling coordinated F and G protein expression that may better mimic natural viral antigen presentation (Fig. 1b and c). All LNP formulations exhibited optimal physicochemical properties. The mRNA-F-LNP showed a size of 98.86 nm with a polydispersity index (PDI) of 0.094, mRNA-G-LNP showed a size of 96.74 nm with a PDI of 0.143, and mRNA-GF-LNP showed a size of 97.3 nm and a PDI of 0.115. These results confirmed consistent nanoparticle formulation (size range: 80–100 nm, PDI < 0.2) across all three formulations. In vitro characterization in HEK293T cells confirmed successful protein expression and proper membrane localization, as validated by western blotting (WB) and immunofluorescence assays (IFA) (Fig. 1d and e).

Three mRNA vaccines elicit robust immune responses in mice

To evaluate NiV-specific antibody responses, 6–8-week-old female SPF BALB/c mice (n = 9) were immunized intramuscularly with 5 μg of mRNA-F-LNP, mRNA-G-LNP, or mRNA-GF-LNP. A prime-boost regimen was employed, with a booster dose administered at day 21 post-primary immunization (Fig. 2a). Serum samples were collected weekly from day 7 to day 42 and then biweekly until day 98 for analysis by ELISA and pseudovirus neutralization assays.

ELISA results revealed that G-specific antibodies emerged as early as day 7 in both the mRNA-G-LNP and mRNA-GF-LNP groups, whereas F-specific antibodies became detectable at day 14 in the mRNA-F-LNP and mRNA-GF-LNP groups (Fig. 2b–e). Following booster immunization, antibody titers against both glycoproteins increased significantly, peaking ($\sim 10^5$) by day 42. The mRNA-GF-LNP group elicited F- and G-specific antibody titers comparable to those induced by the mRNA-F-LNP and mRNA-G-LNP groups, respectively. All vaccine formulations maintained high antibody titers through the end of the observation period (day 98).

Pseudovirus neutralization assays revealed distinct kinetic profiles (Fig. 2f). Neutralizing antibodies were initially detected only in the mRNA-GF-LNP group at day 7. By day 21, all vaccines elicited measurable neutralizing antibodies, with mRNA-GF-LNP showing significantly higher titers than mRNA-F-LNP ($P < 0.01$) and titers equivalent to mRNA-G-LNP. Peak neutralization titers (NT) ($\sim 10^4$) were achieved by day 42 across all groups, with no significant differences observed at this time point.

To assess NiV-specific T cell responses, IFN-γ ELISpot assays were performed on splenocytes collected 21 days after the second immunization. All three vaccines induced robust cellular immune responses. Following F protein stimulation, the mRNA-GF-LNP group exhibited significantly higher IFN-γ production than the mRNA-F-LNP group ($P < 0.05$). In contrast, G protein-induced IFN-γ levels were similar between the mRNA-GF-LNP and mRNA-G-LNP groups (Fig. 2g).

All three mRNA vaccines elicit antigen-specific antibodies in Syrian hamsters

Prior to challenge experiments, we evaluated the immunogenicity of the three mRNA vaccines in Syrian hamsters. 5–6-week-old female Syrian hamsters (n = 15) were randomly divided into four groups: the mRNA-F-LNP, mRNA-G-LNP, mRNA-GF-LNP, and control groups. Syrian hamsters received prime immunization (10 μg each) followed by an identical booster dose at day 21 via intramuscularly injection. The control group received PBS (Fig. 3a). Serum samples were collected for antibody analysis.

Serological analysis showed that all vaccinated groups developed detectable F- and G-specific antibodies by day 21 after the primary immunization, with antibody titers reaching approximately 10^3. Following boosting immunization, we observed robust antibody responses, with antibody titers increasing approximately 10-fold to $\sim 10^4$ by day 28. These elevated antibody levels persisted throughout the 91-day observation period (Fig. 3b–e). Similar to the immunogenicity patterns in mice, Syrian hamsters exhibited consistent antibody kinetics across all vaccine formulations. All groups showed similar antibody responses against both F and G proteins, with synchronized peak responses following booster immunization.

Pseudovirus neutralization profiles in hamsters shared similar features with those in mice (Fig. 3f), with early responses (day 7) in the mRNA-GF-LNP group and delayed neutralization (day 21) detected in the mRNA-G-LNP and mRNA-F-LNP groups. All groups reached similar neutralizing titers by day 42. In live virus neutralization assays, sera from all vaccinated hamsters effectively neutralized both NiV-M and NiV-B, with peak titers reaching approximately 10^3. Notably, the mRNA-GF-LNP and mRNA-G-LNP groups induced significantly higher neutralizing antibody titers against NiV-B than the mRNA-F-LNP group ($P < 0.01$ and $P < 0.05$, respectively) (Fig. 3g).

Collectively, these results demonstrate that all three mRNA vaccines elicit durable antibody responses, indicating a strong potential for long-term protective immunity against NiV.

Three mRNA vaccines provide complete protection against lethal NiV challenge in Syrian hamsters

To evaluate vaccine efficacy, we utilized a stringent Syrian hamster model of NiV infection[29–32]. At 21 days post-booster immunization, Syrian hamsters were challenged intraperitoneally with 1000 LD_{50} of NiV-M (Fig. 3a). Clinical outcomes were monitored daily for 21 days post-challenge (d.p.c), with virological analysis performed at 5 d.p.c.

All control animals exhibited progressive weight loss and clinical signs after challenge (Fig. 4a), with mortality onset at 5 d.p.c. (1 deaths by 5 d.p.c., 3 by 6 d.p.c., 1 by 9 d.p.c., and the remaining 1 succumbing at 15 d.p.c). In contrast, all vaccinated Syrian hamsters maintained normal body weight, showed no clinical symptoms, and survived through the 21-day observation period.

To assess the effect of vaccination on viral replication, we analyzed the viral loads in spleen, lung and brain tissues collected from 6 Syrian hamsters per group at 5 d.p.c. Control animals exhibited high viral loads ($>1 \times 10^6$ copies/g) across all examined tissues, whereas no viral RNA was detectable in any vaccinated animals, indicating complete viral clearance. Viral titration assays confirmed these findings, with control tissues yielding titers of 1.4×10^4 $TCID_{50}$/g (lung), 2.8×10^3 $TCID_{50}$/g (spleen), and 60.25 $TCID_{50}$/g

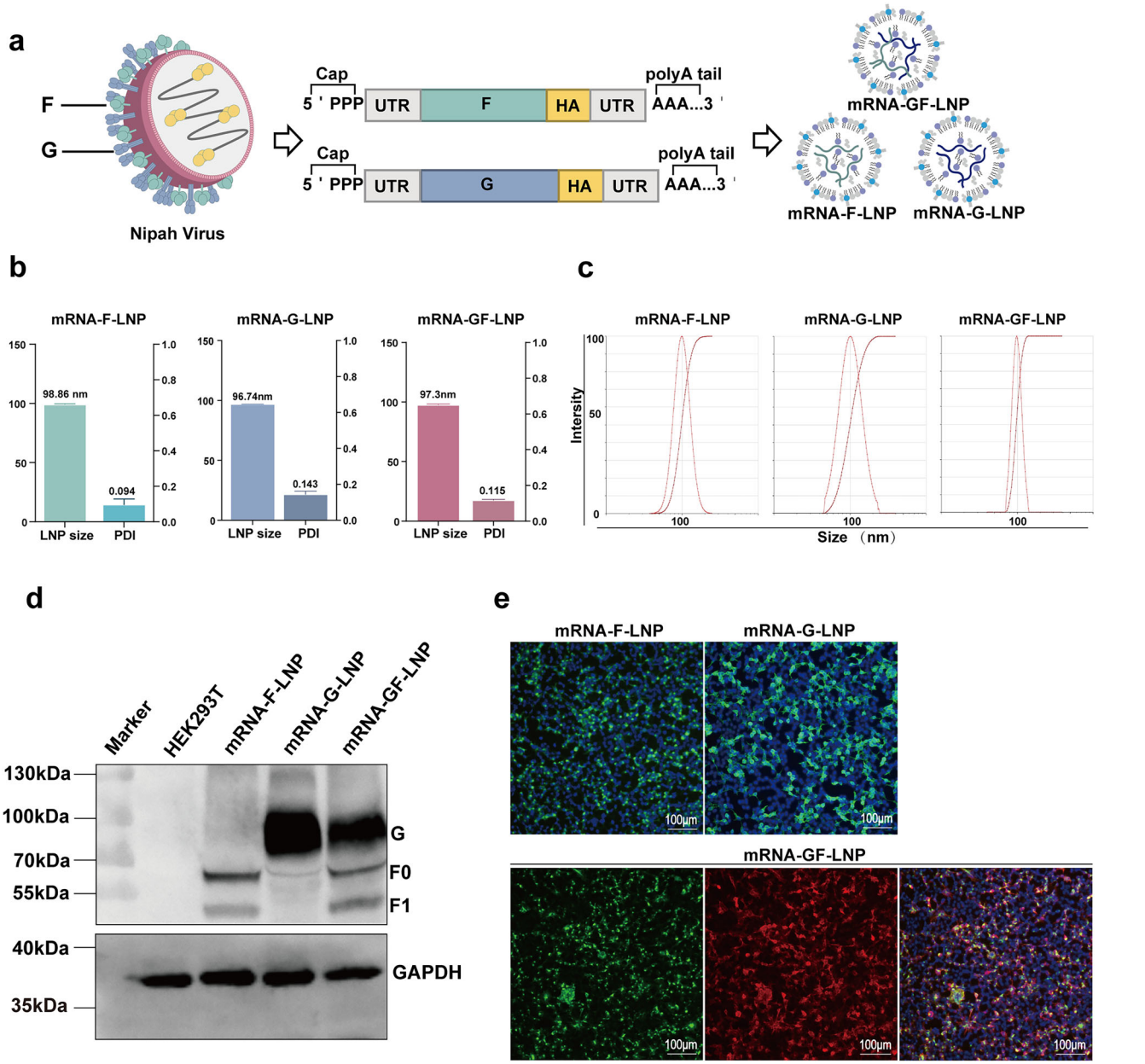

Fig. 1 | Construction and characterization of three mRNA vaccines. a Schematic illustration of mRNA-F and mRNA-G. The mRNAs encoding NiV F and G proteins were synthesized and encapsulated into LNPs to generate three vaccine candidates: mRNA-F-LNP, mRNA-G-LNP, and mRNA-GF-LNP. **b**, **c** Particle size and PDI of the three mRNA-LNP vaccines measured by DLS. All formulations exhibited a uniform particle size distribution (~100 nm) with PDI values below 0.2. **d** Western blot analysis of F and G protein expression in HEK293T cells 48 h post-transfection with mRNA-F-LNP, mRNA-G-LNP or mRNA-GF-LNP. The G protein was detected at ~66 kDa, the F protein was observed as the precursor F0 (~60 kDa) and the cleaved F1 subunit (~48 kDa). GAPDH (~36 kDa) served as a loading control. **e** IFA analysis of F and G protein localization in HEK293T cells 24 h post-transfection. Top panels: cells transfected with mRNA-F-LNP and mRNA-G-LNP, respectively. Bottom panel: cells transfected with mRNA-GF-LNP showing expression of F (green, FITC) and G (red, Alexa Fluor 594) proteins. Scale bar: 100 μm.

(brain) (Fig. 4b). In contrast, no infectious virus was recovered from vaccinated animals. These results demonstrate that all three mRNA vaccine candidates provided complete protection against lethal NiV-M challenge.

All three mRNA vaccines prevented pathological damage after NiV infection

To further evaluate the protective efficacy of the mRNA vaccine candidates against NiV-induced tissue damage, we performed histopathological and immunohistochemical (IHC) analyses of lung, spleen, and brain tissues collected at 5 d.p.c. Histopathological analyses showed that the control group displayed characteristic pathological manifestations of NiV infection. Lung exhibited extensive hyperplasia, diffuse hemorrhage, alveolar collapse, and marked thickening of alveolar septa attributable to vascular congestion, and inflammatory infiltration; Brain showed prominent perivascular cuffing, and lymphocytic infiltration; Spleen showed significant reduction in follicular size, lymphocyte depletion in white pulp, and increased macrophage infiltration (Fig. 5a). In contrast, vaccinated groups showed no evident pathological alterations. Subsequent IHC analysis of NiV nucleoprotein (N) antigen confirmed these findings. The control tissues displayed abundant diffuse viral antigen distribution across all examined tissues, whereas vaccinated animals showed no detectable viral antigen (Fig. 5b).

Taken together, these data demonstrate that the mRNA-F-LNP, mRNA-G-LNP, and mRNA-GF-LNP vaccines effectively eliminate viral

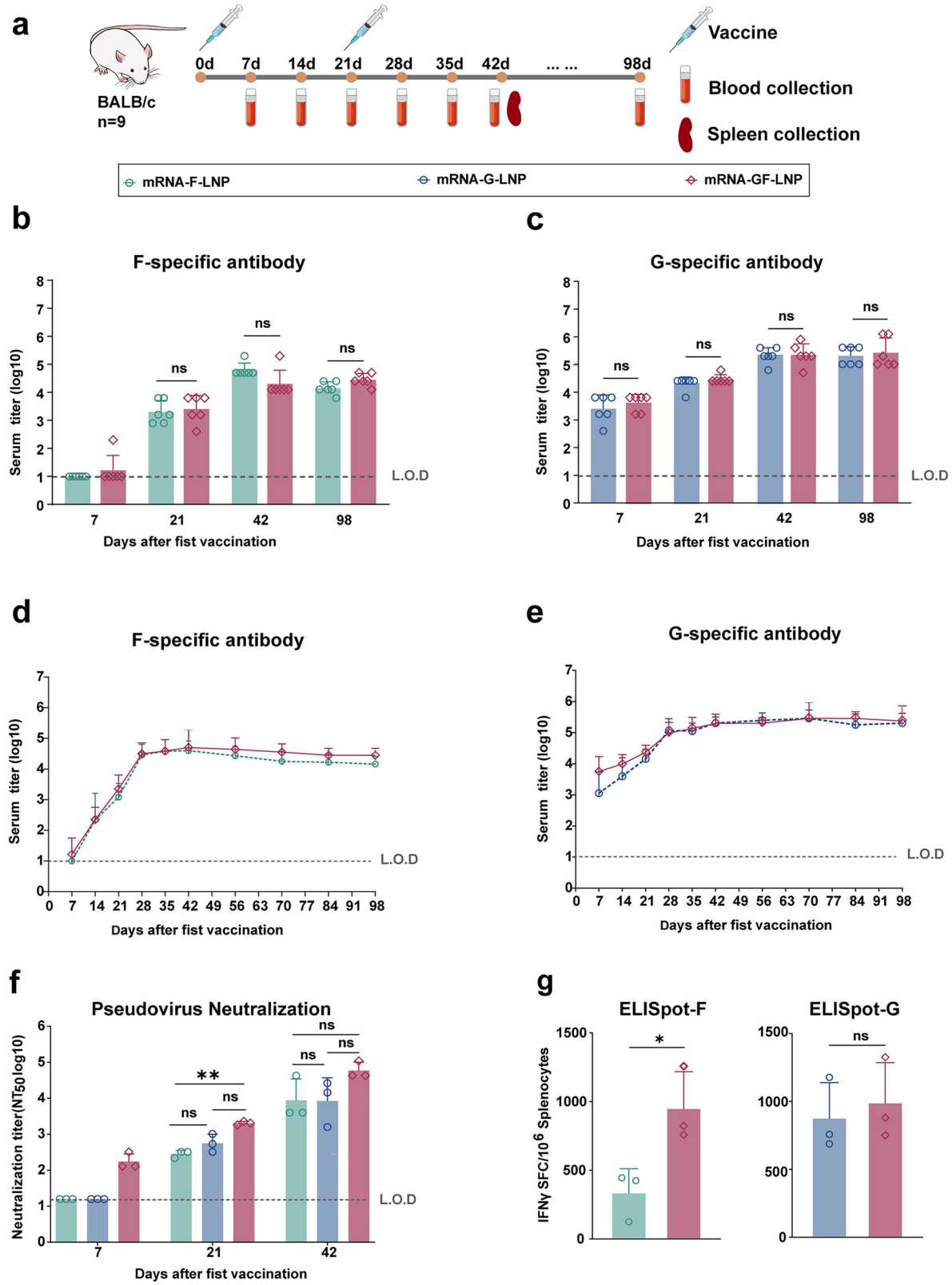

Fig. 2 | Three mRNA vaccines induce potent immune responses in mice. **a** Immunization schedule in mice. Mice received a prime (day 0) and a booster (day 21) intramuscular injection of 5 μg per dose. **b**, **c** The F- and G-specific antibody titers of the sera from mice immunized with mRNA-G-LNP, mRNA-GF-LNP, or mRNA-F-LNP at 7, 21, 42, and 98 days post immunization. **d**, **e** Kinetics of F- and G-specific antibody titers measured by ELISA. **f** The neutralization antibodies in the sera of mice collected at 7, 21, and 42 days post prime immunization by pseudovirus neutralization assays. **g** IFN-γ production induced by the three vaccines detected by ELISpot at 21 days after the second immunization. Data are presented as mean ± SEM. Statistical significance was determined by one-way ANOVA with Tukey's multiple-comparison test (**b**, **c**, **f**) and Student's two-tailed t-test (**g**). $^{*}P < 0.05$, $^{**}P < 0.01$, ns, not significant. L.O.D. represents limit of detection.

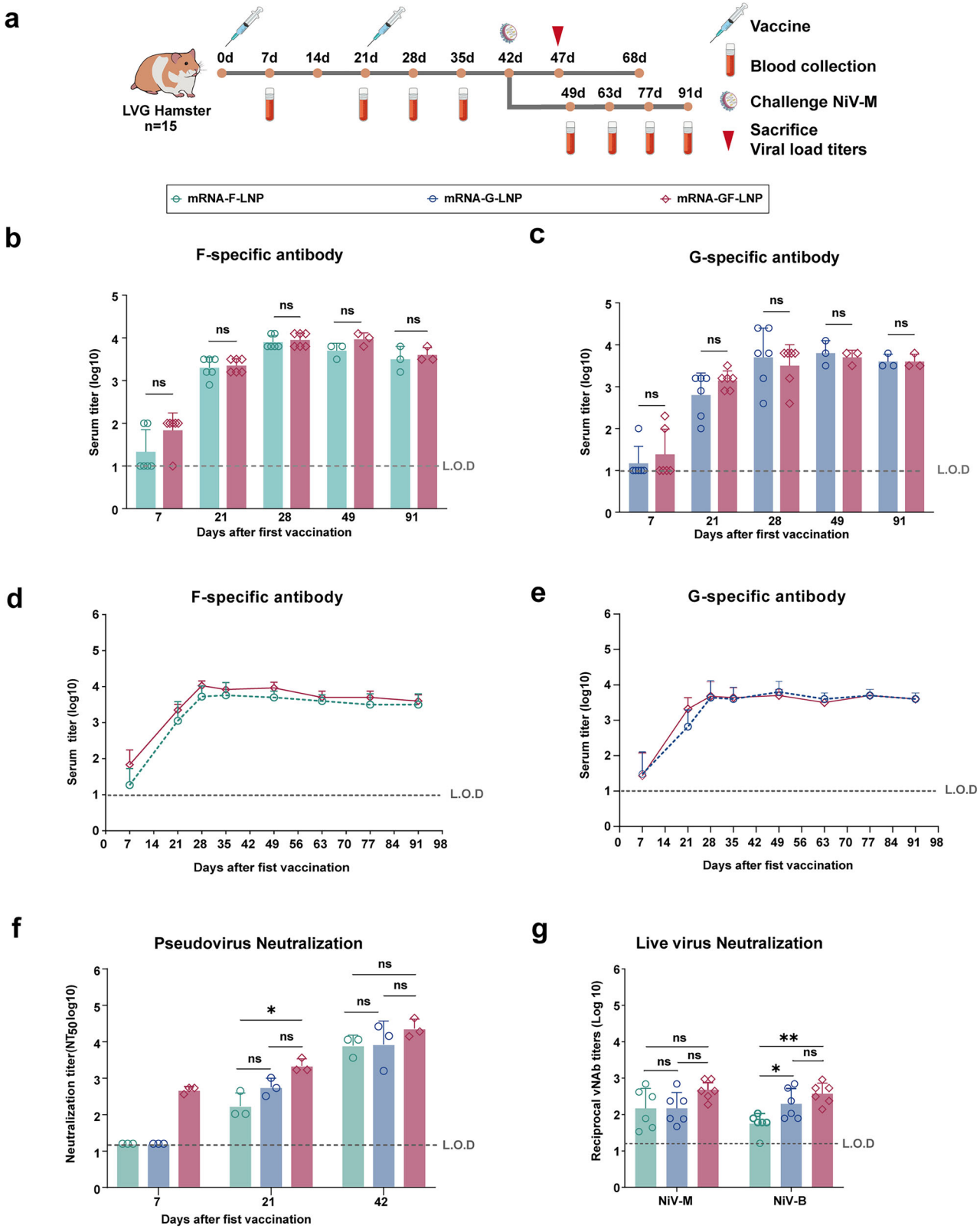

Fig. 3 | Immunogenicity and challenge schedule in Syrian hamster. **a** Immunization and challenge schedule in Syrian hamsters. Syrian hamsters were immunized with 10 μg of mRNA-F-LNP, mRNA-G-LNP, or mRNA-GF-LNP at day 0 and received a booster immunization at day 21. A lethal challenge with NiV-M was performed at 21 days post the booster immunization. **b**, **c** The F- and G-specific antibody titers of the sera from hamster immunized with mRNA-G-LNP, mRNA-GF-LNP, or mRNA-F-LNP at 7, 21, 28, 49, and 91 days post immunization. Antigen-specific antibody kinetics. F-specific **d** and G-specific **e** antibody titers (n = 15, day 7 to 42; n = 3, day 49 to 91). **f** The neutralizing antibodies in the sera of hamsters collected at 7, 21, and 42 days post prime immunization by pseudovirus neutralization assays. **g** Virus-neutralizing antibody (vNAb) detection based on the live NiV-M and NiV-B at 2 weeks after the last immunization. Data are presented as mean ± SEM. Statistical significance was determined by One-way ANOVA with Tukey's multiple-comparison test. $^{*}P < 0.05$, $^{**}P < 0.01$, ns, not significant. L.O.D. represents limit of detection.

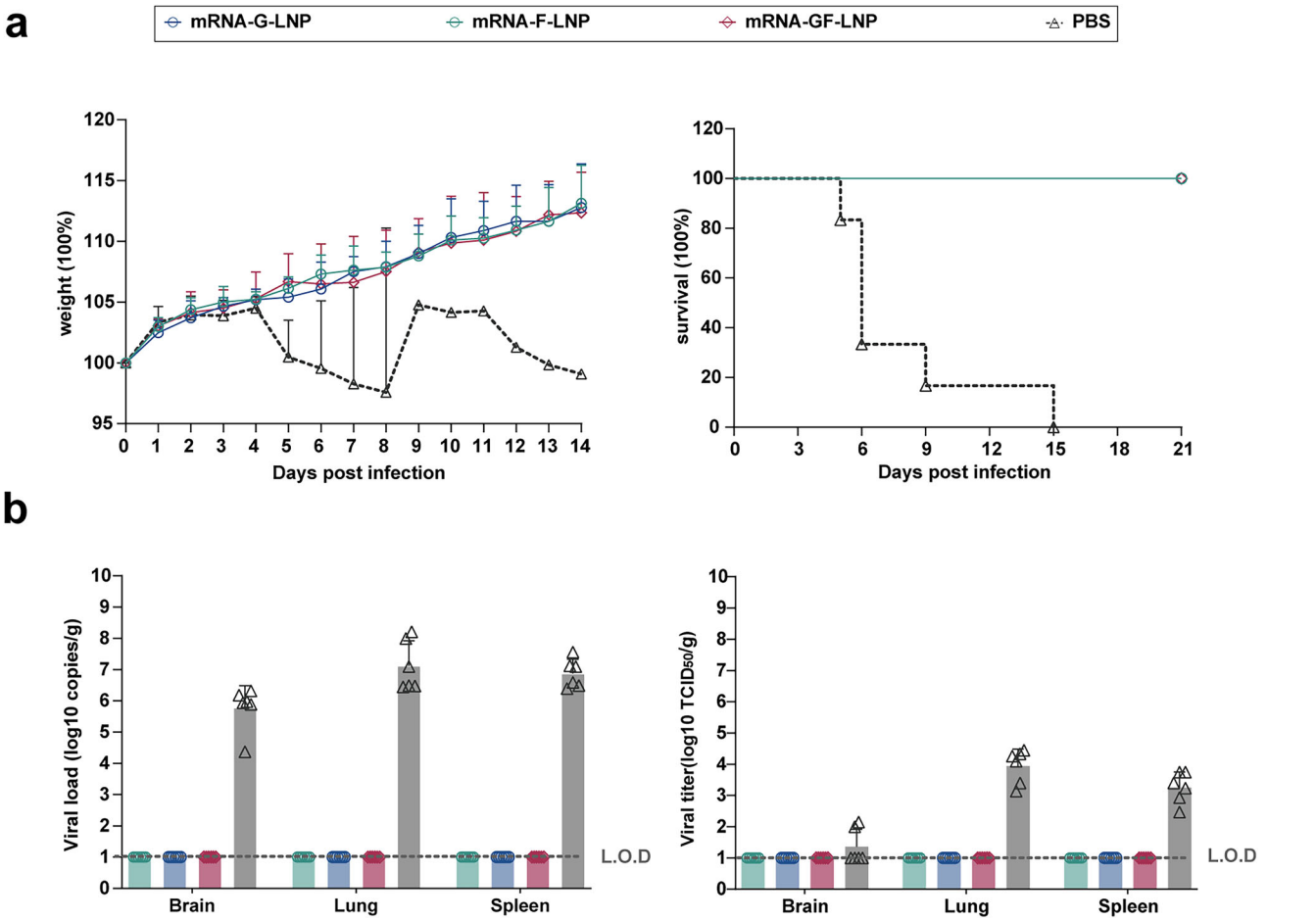

Fig. 4 | Protective efficacy of three mRNA vaccines in Syrian hamsters challenged with NiV-M. a Body weight changes and survival rates of Syrian hamsters following NiV-M challenge at 21 days post the second immunization. **b** Viral loads in brain, lung, and spleen tissues at 5 d.p.c. quantified by qRT-PCR (left panel) and live virus titration (right panel). Data are presented as mean ± SEM. L.O.D. represents limit of detection.

infection, prevent virus-induced tissue pathology damage and inflammation in critical organs, and provide complete protection against lethal NiV challenge in Syrian hamsters.

Discussion

NiV represents a significant zoonotic threat with case fatality rates of approximately 75% in human outbreaks across Southeast Asia[4,33–35]. The lack of approved treatments or vaccines highlight the urgent need for effective prevention strategies. mRNA technology provides advantages for rapid response to emerging pathogens, featuring simplified production and improved safety profiles[36,37]. In this study, we designed mRNA vaccines targeting the NiV F and G proteins and investigated their protective efficacy in Syrian hamsters.

First, the full-length F and G protein sequences were cloned into plasmids containing the 5' and 3' UTRs. After in vitro transcription and capping, mRNA-G and mRNA-F were obtained. These mRNAs were encapsulated into LNPs containing SM-102 lipid, known to promote efficient cellular uptake and endosomal escape[38–40]. Following LNP encapsulation, mRNA-G-LNP and mRNA-F-LNP were prepared. A previous study has shown that chimeric F/G constructs enhanced neutralizing antibody titers[41]. To potentially mimicking natural viral antigen presentation, mRNA-G and mRNA-F were co-encapsulated into LNP, generating mRNA-GF-LNP. Three mRNA vaccine candidates were expressed in HEK293T cells.

Immunogenicity evaluation showed distinct response patterns between the glycoproteins. All three vaccine formulations induced similar antigen-specific antibody titers in mice and Syrian hamsters, with no immunogenicity advantage for the co-formulated vaccine. This phenomenon may be dose-dependent, as 5 μg vaccination dose falls within the 1–10 μg range where mRNA vaccines often show minimal differences in humoral responses[42,43]. Previous studies suggest that immunogenicity differences become more pronounced at lower doses (<0.1 μg), indicating that dose optimization might reveal advantages of the mRNA-GF-LNP[42,43]. These results align with prior vaccinia virus-vectored vaccine study (VV-NiV.G and VV-NiV.F) where co-immunization failed to enhance antibody responses compared to individual immunization[22].

Notably, F-specific antibodies (from mRNA-F-LNP and mRNA-GF-LNP) became detectable at 14 d.p.i., reaching approximately 10^3 by day 21. In contrast, G-specific antibodies (from mRNA-G-LNP and mRNA-GF-LNP) achieved titers of approximately 10^3 as early as 7 d.p.i. Previous research has also shown that prefusion-based mRNA vaccine exhibited higher neutralizing activity than post-fusion versions[42], suggesting protein stability, pre-fusion conformation maintenance, and neutralizing epitope preservation may critically influence immunogenicity. This delayed F-specific antibodies might be caused by this reason or its relatively lower expression levels. Despite these differences, all formulations ultimately produced strong and sustained antibody titers (~10^5) throughout the 98-day observation period. Additionally, all three candidates elicited strong antigen-specific T-cell responses in mice. Notably, mRNA-GF-LNP triggered significantly higher IFN-γ production than mRNA-F-LNP upon F protein stimulation, whereas G-specific T-cell responses were comparable between mRNA-GF-LNP and mRNA-G-LNP.

Pseudovirus neutralization assays revealed the advantage of mRNA-GF-LNP, generating detectable neutralization by 7 d.p.i. and significantly higher titers than mRNA-F-LNP at 21 d.p.i., suggesting the synergistic

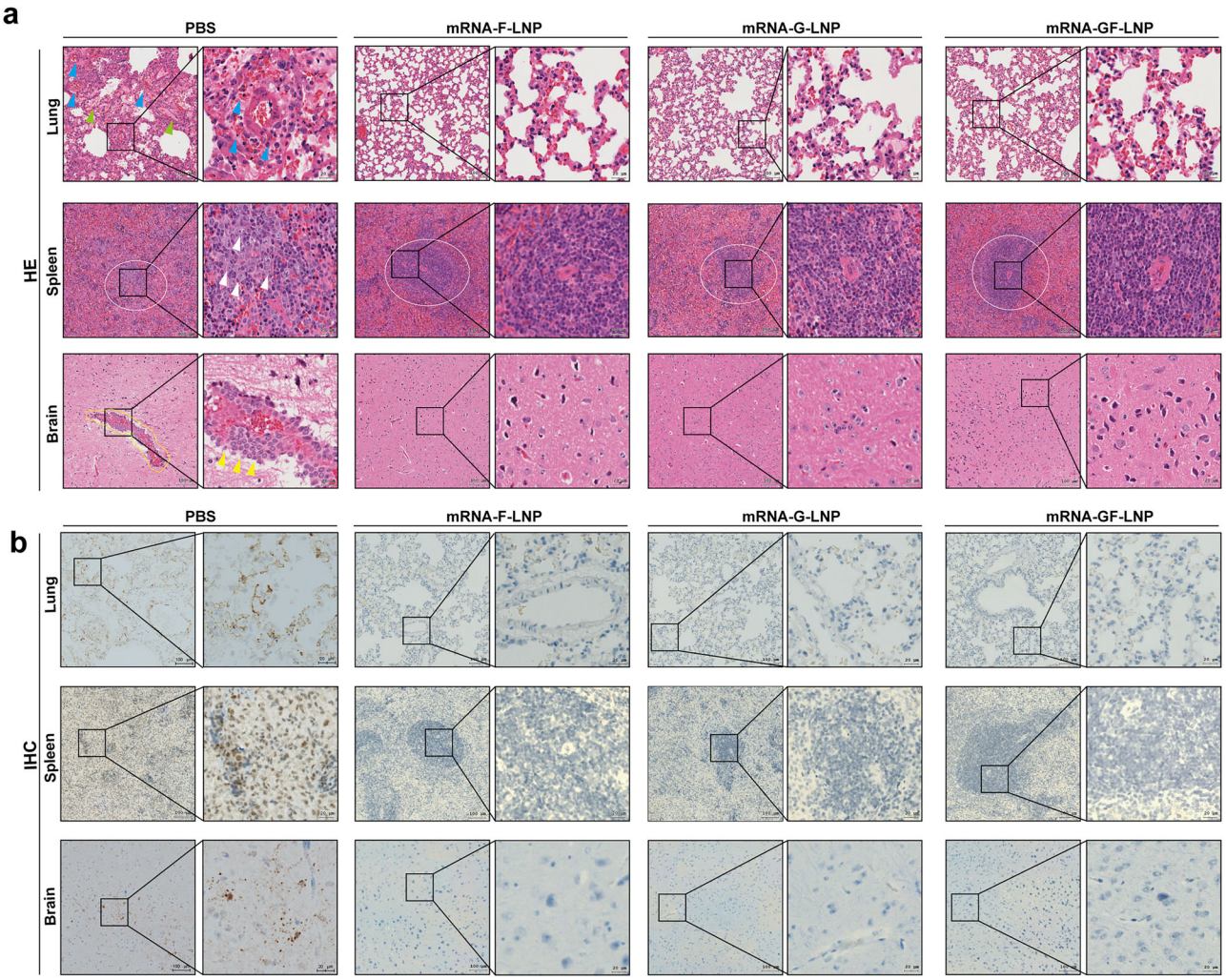

Fig. 5 | Pathological changes in tissues of Syrian hamsters challenged with NiV-M. a Hematoxylin and eosin (H&E) staining of tissue sections: Comparison between control group (PBS-injected) and vaccinated groups (mRNA vaccine-injected) at 5 d.p.c. Lung: Fibrinous exudates (green triangles), hemorrhage (blue triangles). Spleen: Increased macrophages (white triangles), lymphoid follicles (circled in white). Brain: Perivascular cuffing (yellow outlines), lymphocytic infiltration (yellow triangles). **b** IHC staining for NiV N antigen: Viral antigen appears as brownish-red deposits. No NiV antigen was detected in vaccinated groups, whereas diffuse viral antigen was observed in lung, spleen, and brain tissues of control animals. Magnification: 5× (scale bar: 100 μm), 20× (scale bar: 20 μm).

effects between G and F proteins. After boosting, all vaccines achieved similar neutralization titers (~10^4). In live virus neutralization assays, sera from all immunized Syrian hamsters neutralized NiV-M and NiV-B viruses. Challenge studies showed Syrian hamsters immunized with any of the three mRNA vaccine candidates were completely protected against lethal NiV-M challenge. Control group showed significant weight loss by 5 d.p.c. and ultimately succumbed, all vaccinated Syrian hamsters maintained normal weight and survived. Pathological and IHC analyses revealed no detectable lesions or viral antigen in brain, lung, or spleen tissues from immunized groups.

Although this study demonstrates the protective efficacy of the mRNA-LNP candidates against NiV challenge in hamsters, several limitations should be acknowledged. The protective efficacy of these vaccines remains to be evaluated in other susceptible species, such as pigs and non-human primates, which is essential for assessing their broad applicability. While the vaccine dose used in this study provided complete protection, dose-ranging studies are needed to determine the optimal immunization regimen for future development.

In conclusion, we designed mRNA-F and mRNA-G targeting NiV F and G proteins. Through individual and combined LNP encapsulation, we developed three mRNA vaccines candidates: mRNA-F-LNP, mRNA-G-LNP, and mRNA-GF-LNP. All three vaccines induced high-titer specific and neutralizing antibodies in mice and Syrian hamsters. In challenge experiments, all vaccines provided complete protection against lethal NiV-M infection in Syrian hamsters, demonstrating their potential utility for NiV prevention.

Methods

Cells and viruses

HEK293T and Vero cells were cultured in complete DMEM (contain 10% fetal bovine serum (FBS) (PAN-Biotech). Cells were cultured at 37 °C in a 5% CO_2 atmosphere. The NiV-M and NiV-B used in this study was provided and handled by the National Virus Resource Center, Wuhan Institute of Virology, Chinese Academy of Sciences.

Preparation of NiV mRNA vaccines

The F and G gene sequences of the NiV-M (GenBank: AJ627196.1) were retrieved from NCBI and codon-optimized. Following optimization, the sequences were flanked with 5' and 3' UTRs and cloned into the pcDNA3.1 vector downstream of the T7 promoter (Sangon Biotech, Shanghai). For mRNA production, template DNA was amplified by PCR using 2× KeyPo SE Master Mix (Vazyme) with primers containing T7 promoter sequence (forward) and poly(T) plus partial 5' UTR sequence (reverse). Following gel purification, the amplification

product was subjected to in vitro transcription using T7 RNA polymerase, followed by the addition of the Cap1 Analog (APExBIO, USA). mRNA was then purified using the MEGAclear™ Kit (Thermo Fisher), yielding final mRNA-F and mRNA-G products.

LNP encapsulation of NiV mRNA vaccines

The mRNA-F and mRNA-G were encapsulated into LNPs using the following standardized protocol: the aqueous phase was prepared by diluting mRNA solution with nuclease-free water to 180 μg/mL, followed by addition of citrate buffer (10 mM, pH 3.0) to achieve a final mRNA concentration of 90 μg/mL; and the lipid phase consisted of SM-102 (MedChemExpress), 1,2-DSPC (MedChemExpress), cholesterol, and DMG-PEG (2000) (MedChemExpress) dissolved in ethanol (Sinopharm Chemical Reagent Co., Ltd) at a molar ratio of 50:10:38.5:1.5. The two phases were mixed at a 1:3 using a microfluidic chip device (Micro&Nano Co., Ltd) to generate three formulations: mRNA-F-LNP, mRNA-G-LNP, and mRNA-GF-LNP (co-encapsulating both mRNAs at 1:1 molar ratio). LNP characteristics were assessed by dynamic light scattering (DLS).

Western blot analysis

HEK293T cells were cultured in 6-well plates (NEST) and incubated with 2 μg of mRNA-F-LNP, mRNA-G-LNP, or mRNA-GF-LNP. The samples were collected after 48 h, denatured in 5× SDS loading buffer at 70 °C for 10 min, and then resolved by 10% SDS-PAGE, the proteins were transferred to a membrane, which was blocked prior to antibody incubation: anti-HA-Tag (6E2) mouse monoclonal antibody (1:1000) (Cell Signaling Technology, CST) and anti-GAPDH polyclonal antibody (1:5000) (Proteintech) conducted at 4 °C for 16–18 h. The membranes were washed with PBST and incubated with HRP-conjugated secondary antibody (CST) (1:5000, 1 h at room tempurature (RT)). Protein bands were developed using chemiluminescent substrate (Yeasen Biotechnology) and visualized by UVP Chemsolo Auto (Analytik Jena). Uncropped and unprocessed original scans are provided in Supplementary Fig. 1.

Immunofluorescence analysis

When HEK293T cells achieved 70–80% confluency in 96-well plates, they were transfected with mRNA-F-LNP, mRNA-G-LNP, or mRNA-GF-LNP (100 ng per well). Following 24 h transfection, the cells were fixed with anhydrous ethanol (15 min at RT). Following fixation, the cells were blocked with 5% skim milk (1 h at 37 °C). For mRNA-F-LNP or mRNA-G-LNP expression, the cells were incubated with mouse polyclonal antisera specific to F or G protein (1:500, 37 °C for 1 h). After washing with PBST, the cells were incubated with FITC-conjugated anti-mouse IgG secondary antibody (1:2000) (BioLegend) (37 °C for 1 h). Nuclei were then counterstained with DAPI (1:10,000) (Beyotime) (15 min, RT). For mRNA-GF-LNP expression, after blocking and washing, sequential incubations were performed: first with mouse anti-F polyclonal serum (1:500, 37 °C, 1 h), followed by PBST washes, the cells were incubated with pig anti-G polyclonal serum (1:500, 1 h at 37°). Following a wash step, the cells were probed with FITC-conjugated anti-mouse IgG antibody (1:2000) and AF594-conjugated goat anti-pig IgG (HL) antibody (1:500; Abmart), respectively (1 h at 37 °C). Finally, cells were counterstained with DAPI as described above. Expression of G and F proteins were examined using a fluorescence microscope (ZEISS).

Animal experiments

Thirty-six female BALB/c mice (aged 6-8 weeks) were randomly divided into four groups (n = 9) (SiPeiFu (Suzhou)). Animals received intramuscular immunization with 5 μg of either mRNA-GF-LNP, mRNA-F-LNP, or mRNA-G-LNP, and the control group were injected with 100 μL PBS. All animals were immunized twice with a 21-day interval between doses. Serum samples were collected weekly starting at day 7 post-primary immunization through day 98 for serum antibody monitoring. Mice were anesthetized using 4% isoflurane (RWD Life Science) before blood sampling. Upon completion of the experimental procedures, all mice were euthanized humanely using carbon dioxide inhalation followed by cervical dislocation. Carbon dioxide was introduced into a sealed chamber at a flow rate that displaced 30% of the chamber volume per minute.

Four experimental groups (n = 15; a total of sixty) were established by randomly assigning SPF female Syrian hamsters (5–6 weeks old, Beijing Vital River Laboratory Animal Technology Co., Ltd). Three immunization groups received 10 μg of mRNA-GF-LNP, mRNA-F-LNP, or mRNA-G-LNP intramuscularly, while controls received 200 μL of PBS. Following two immunizations (21-day interval), randomly selected animals (n = 12 per group) were transferred to ABSL-4 facilities and challenged with 1000 LD_{50} of NiV-M via intraperitoneal route. Six per group were euthanized at 5 d.p.c., lung, spleen, and brain tissues were collected for subsequent viral load quantification and histopathological analysis. The remaining six hamsters per group were monitored for body weight changes through 14 d.p.c. and survival through 21 d.p.c. An additional three hamsters per group were maintained for extended antibody monitoring until day 91. At the end of the experiment, all hamsters were euthanized by carbon dioxide inhalation. All animal studies follow the ARRIVE guidelines[44].

ELISA

Antibody levels in mouse and hamster serum samples were detected by an indirect ELISA. Briefly, 96-well microplates (NEST) were coated with either NiV Pre-Fusion glycoprotein (ACRO Biosystems) or NiV G Protein (Novoprotein). The blocked plates were incubated with serially diluted serum samples (starting at 1:100, 1 h at 37 °C). After further PBST washes, species-specific HRP-conjugated secondary antibodies: anti-mouse IgG-HRP (1:5000) (CST) or goat anti-hamster IgG-HRP (1:10,000) (Abcam) were added and incubated at 37 °C for 45 min. Plates were washed again and developed with TMB substrate solution (TIANGEN) (37 °C, 15 min) in the dark. The reactions were stopped with 2 M H_2SO_4, and optical density at 450 nm (OD_{450}) was measured using a microplate reader (Biotek).

Enzyme-linked immune absorbent spot (ELISpot) assay

Splenocytes were adjusted to appropriate density in serum-free medium and plated at 5×10^5 cells per well in 100 μL onto pre-coated mouse IFN-γ ELISpot plates (Mabtech). The cells were stimulated with 5 μg/mL of either G or F protein. Concanavalin A (ConA, 5 μg/mL) and serum-free medium were used as positive and negative controls, respectively. Following incubation, spot-forming units (SFU) were quantified as counts per million cells using AT-Spot™ ELISpot Image Analysis System (Antai Yongxin Tech (Guangzhou) Co., Ltd).

Pseudovirus neutralization assay

Neutralizing antibody responses were evaluated using a pseudotyped virus system. Pseudoviruses were generated by co-transfecting HEK293T cells (70% confluency in T75 flasks) with the following plasmids at optimized ratio (6:11:1:2): pLOV-CMV-GFP, pSPAX2, pcDNA3.1-F, and pcDNA3.1-G. The total DNA mixture (35 μg) was incubated with 70 μL PEI transfection reagent for 20 min at RT and then added to cells. Following 48 h transfection, the supernatant was harvested and centrifuged at 300 × *g* for 5 min. The clarified supernatant, designated as the pseudotyped virus, was aliquoted and stored at −80 °C.

After inactivation (56 °C, 30 min), the serum was first diluted 1:20, and a threefold serial dilution was subsequently performed. Sera were mixed with 200 $TCID_{50}$ of pseudovirus and incubated at 37 °C for 1.5 h. The mixtures (100 μL) were then added to HEK293T cells. After 48 h incubation, GFP-positive wells were counted, and neutralizing antibody titers (NT) were calculated using the Reed-Muench method.

Live virus neutralization assay

Serum from Syrian hamsters collected at 14 days post-second immunization have been inactivated (56 °C, 30 min). Using DMEM supplemented with 2% FBS, the serum was subjected to three-fold serial dilutions starting from 1:20. The diluted serum was mixed with 100 $TCID_{50}$ of NiV-M or NiV-B and incubated at 37 °C for 1 h. The mixture was inoculated onto Vero E6 cells (four replicates per dilution). After 1 h incubation at 37 °C, the

inoculum was replaced with complete DMEM and the cells were cultured for 5 days. Cytopathic effect (CPE) was recorded daily. The neutralizing antibody titer was calculated (the highest serum dilution that provided complete protection to 50% of the cell monolayers).

qRT-PCR

qRT-PCR was performed to quantify the viral loads in hamster tissues as previously described[45]. Briefly, lung, spleen, and brain tissues were collected from Syrian hamsters at 5 d.p.c. for RNA extraction. The NiV N gene was amplified using a TaqMan probe-based assay on a CFX96 Real-Time System (Bio-Rad) with the HiScript II One Step qRT-PCR Probe Kit (Vazyme). The used primers and probe were: forward primer: 5'-AACATCAGCAGGAAGGCAAGA-3', reverse primer: 5'-GCCACTCTGTTCTATAGGTTCTTC-3', and probe: FAM-5'-TTGCTGCAGGAGGTGTGCTC-BHQ1-3'. A standard curve was generated to calculate the N gene copy number.

Virus titration assay

Tissue homogenates were subjected to10-fold serial dilutions in DMEM supplemented with 2% FBS, and 100 μL of each dilution were then applied to Vero E6 cell monolayers and incubated at 37 °C under 5% CO_2 for 1 h, the culture was removed, and the cells were maintained in DMEM containing 2% FBS for 5 days, and final CPE scoring at day 5 was used to calculate viral titers (log10 $TCID_{50}$/g) using the Reed-Muench method.

Histopathological and immunohistochemical analysis

Following challenge infection, the lung, brain, and spleen from Syrian hamsters were collected and fixed in 10% paraformaldehyde solution for 7 days. After embedding in paraffin, tissue samples were sectioned at a thickness of 4 μm and subsequently stained with H&E. For IHC analysis, an in-house developed monoclonal antibody specific for NiV N protein was used. The sections were scanned using a Pannoramic MIDI system (ZEISS).

Statistical analysis

All data were analyzed using GraphPad Prism software (version 10.4) and presented as mean ± SEM. Statistical differences were assessed using one-way analysis of variance (ANOVA) and Student's two-tailed t-test. Statistical significance was set at $P < 0.05$. ns, not significant, $^{*}P < 0.05$, $^{**}P < 0.01$.

Ethic statement

The immunization studies in mice and hamsters complied with the ethical guidelines approved by the Animal Ethics Committee of the Shanghai Veterinary Research Institute, Chinese Academy of Agricultural Sciences (Approval Nos.: SV-20240607-03 and SV-20241018-01). All NiV challenge experiments were performed under Animal Biosafety Level 4 (ABSL-4) facility at the National Biosafety Laboratory (Wuhan), Chinese Academy of Sciences, with protocols approved by the Institutional Animal Care and Use Committee (Approval No.: WIVA21202402).

Data availability

The data that support the findings of this study are available from the corresponding author upon reasonable request.

Received: 13 August 2025; Accepted: 2 December 2025;
Published online: 19 December 2025

References

1. Paliwal, S., Shinu, S. & Saha, R. An emerging zoonotic disease to be concerned about - a review of the nipah virus. *J. Health Popul. Nutr.* **43**, 171 (2024).
2. Amal, N. M. et al. Risk factors for Nipah virus transmission, Port Dickson, Negeri Sembilan, Malaysia: results from a hospital-based case-control study. *Southeast Asian J. Trop. Med. Public Health* **31**, 301–306 (2000).
3. Enserink, M. Emerging diseases. Malaysian researchers trace Nipah virus outbreak to bats. *Science* **289**, 518–519 (2000).
4. Ajith Kumar, A. K. & Anoop Kumar, A. S. Deadly Nipah Outbreak in Kerala: Lessons Learned for the future. *J. Crit. Care Med.* **22**, 475–476 (2018).
5. AbuBakar, S. et al. Isolation and molecular identification of Nipah virus from pigs. *Emerg. Infect. Dis.* **10**, 2228–2230 (2004).
6. Mills, J. N. et al. Nipah virus infection in dogs, Malaysia, 1999. *Emerg. Infect. Dis.* **15**, 950–952 (2009).
7. Qiu, X., Wang, F. & Sha, A. Infection and transmission of henipavirus in animals. *Comp. Immunol. Microbiol. Infect. Dis.* **109**, 102183 (2024).
8. Thiagarajan, K. Nipah virus: Kerala reports second death in four months. *BMJ* **386**, q2058 (2024).
9. Bruno, L. et al. Nipah Virus disease: epidemiological, clinical, diagnostic and legislative aspects of this unpredictable emerging zoonosis. *Animals* **13**, 159 (2022).
10. Satter, S. M. et al. Tackling a global epidemic threat: Nipah surveillance in Bangladesh, 2006-2021. *PLoS Negl. Trop. Dis.* **17**, e0011617 (2023).
11. Eaton, B. T., Broder, C. C., Middleton, D. & Wang, L. F. Hendra and Nipah viruses: different and dangerous. *Nat. Rev. Microbiol.* **4**, 23–35 (2006).
12. Bowden, T. A. et al. Structural basis of Nipah and Hendra virus attachment to their cell-surface receptor ephrin-B2. *Nat. Struct. Mol. Biol.* **15**, 567–572 (2008).
13. Pernet, O., Wang, Y. E. & Lee, B. Henipavirus receptor usage and tropism. *Curr. Top. Microbiol. Immunol.* **359**, 59–78 (2012).
14. Ang, L. T. et al. Generating human artery and vein cells from pluripotent stem cells highlights the arterial tropism of Nipah and Hendra viruses. *Cell* **185**, 2523–2541.e30 (2022).
15. Bossart, K. N., Fusco, D. L. & Broder, C. C. Paramyxovirus entry. *Adv. Exp. Med. Biol.* **790**, 95–127 (2013).
16. Stone, J. A., Vemulapati, B. M., Bradel-Tretheway, B. & Aguilar, H. C. Multiple strategies reveal a Bidentate Interaction between the Nipah virus attachment and fusion glycoproteins. *J. Virol.* **90**, 10762–10773 (2016).
17. Mire, C. E. et al. Single injection recombinant vesicular stomatitis virus vaccines protect ferrets against lethal Nipah virus disease. *Virol. J.* **10**, 353 (2013).
18. Mire, C. E. et al. Use of single-injection recombinant vesicular stomatitis virus vaccine to protect nonhuman primates against lethal Nipah Virus disease. *Emerg. Infect. Dis.* **25**, 1144–1152 (2019).
19. Foster, S. L. et al. A recombinant VSV-vectored vaccine rapidly protects nonhuman primates against lethal Nipah virus disease. *Proc. Natl. Acad. Sci. USA* **119**, e2200065119 (2022).
20. DeBuysscher, B. L., Scott, D., Thomas, T., Feldmann, H. & Prescott, J. Peri-exposure protection against Nipah virus disease using a single-dose recombinant vesicular stomatitis virus-based vaccine. *NPJ Vaccines* **1**, 16002 (2016).
21. Weingartl, H. M. et al. Recombinant nipah virus vaccines protect pigs against challenge. *J. Virol.* **80**, 7929–7938 (2006).
22. Guillaume, V. et al. Nipah virus: vaccination and passive protection studies in a hamster model. *J. Virol.* **78**, 834–840 (2004).
23. Ploquin, A. et al. Protection against henipavirus infection by use of recombinant adeno-associated virus-vector vaccines. *J. Infect. Dis.* **207**, 469–478 (2013).
24. Yoneda, M. et al. Recombinant measles virus vaccine expressing the Nipah virus glycoprotein protects against lethal Nipah virus challenge. *PloS ONE* **8**, e58414 (2013).
25. Mire, C. E. et al. A recombinant Hendra virus G glycoprotein subunit vaccine protects nonhuman primates against Hendra virus challenge. *J. Virol.* **88**, 4624–4631 (2014).
26. Rahman, M. M. et al. An immunoinformatics prediction of novel multi-epitope vaccines candidate against surface antigens of Nipah Virus. *Int. J. Pept. Res. Ther.* **28**, 123 (2022).
27. Spengler, J. R. et al. Henipaviruses: epidemiology, ecology, disease, and the development of vaccines and therapeutics. *Clin. Microbiol. Rev.* **38**, e0012823 (2025).

28. Hassett, K. J. et al. Optimization of lipid nanoparticles for intramuscular administration of mRNA Vaccines. *Mol. Ther. Nucleic Acids* **15**, 1–11 (2019).
29. Wong, K. T. et al. A golden hamster model for human acute Nipah virus infection. *Am. J. Pathol.* **163**, 2127–2137 (2003).
30. De Wit, E. et al. Nipah virus transmission in a hamster model. *PLoS Negl. Trop. Dis.* **5**, e1432 (2011).
31. Rockx, B. et al. Clinical outcome of henipavirus infection in hamsters is determined by the route and dose of infection. *J. Virol.* **85**, 7658–7671 (2011).
32. de Wit, E. et al. Foodborne transmission of nipah virus in Syrian hamsters. *PLoS Pathog.* **10**, e1004001 (2014).
33. Chua, K. B. et al. Fatal encephalitis due to Nipah virus among pig-farmers in Malaysia. *Lancet* **354**, 1257–1259 (1999).
34. Centers for Disease Control and Prevention (C. D. C). Outbreak of Hendra-like virus--Malaysia and Singapore, 1998-1999. *MMWR Morb Mortal Wkly Rep*. **48**, 265-269 (1999).
35. Harcourt, B. H. et al. Genetic characterization of Nipah virus, Bangladesh, 2004. *Emerg. Infect. Dis.* **11**, 1594–1597 (2005).
36. Ferraro, B. et al. Clinical applications of DNA vaccines: current progress. *Emerg. Infect. Dis.* **53**, 296–302 (2011).
37. Carralot, J. P. et al. Polarization of immunity induced by direct injection of naked sequence-stabilized mRNA vaccines. *Cell Mol. Life Sci.* **61**, 2418–2424 (2004).
38. Akinc, A. et al. Targeted delivery of RNAi therapeutics with endogenous and exogenous ligand-based mechanisms. *Mol. Ther.* **18**, 1357–1364 (2010).
39. Yan, X. et al. The role of apolipoprotein E in the elimination of liposomes from blood by hepatocytes in the mouse. *Biochem. Biophys. Res. Commun.* **328**, 57–62 (2005).
40. Binici, B., Rattray, Z., Zinger, A. & Perrie, Y. Exploring the impact of commonly used ionizable and pegylated lipids on mRNA-LNPs: a combined in vitro and preclinical perspective. *J. Control Release* **377**, 162–173 (2025).
41. Loomis, R. J. et al. Structure-based design of Nipah Virus vaccines: a generalizable approach to paramyxovirus immunogen development. *Front. Immunol.* **11**, 842 (2020).
42. Loomis, R. J. et al. Chimeric Fusion (F) and Attachment (G) glycoprotein antigen delivery by mRNA as a candidate Nipah Vaccine. *Front. Immunol.* **12**, 772864 (2021).
43. Corbett, K. S. et al. SARS-CoV-2 mRNA vaccine design enabled by prototype pathogen preparedness. *Nature* **586**, 567–571 (2020).
44. Kilkenny, C. et al. Improving bioscience research reporting: the ARRIVE guidelines for reporting animal research. *PLoS Biol.* **8**, e1000412 (2010).
45. Lu, M. et al. Both chimpanzee adenovirus-vectored and DNA vaccines induced long-term immunity against Nipah virus infection. *NPJ Vaccines* **8**, 170 (2023).

Acknowledgements

This work was supported by the National Key Research and Development Program of China (No. 2022YFD1800500). We thank the National Biosafety Laboratory, Wuhan (CSTR: 31120.02.NBL), Chinese Academy of Sciences, for providing BSL-4 and ABSL-4 facility support for this project.

Author contributions

T.S. and Y.Y. are co-first authors of this publication. H.C., J.L., C.S., Z.Y., and Y.Y. conceived, designed the research. T.S. and C.T. prepared the vaccines. T.S., Z.L., and J.H. performed the mice experiments. Y.Y., Y.P., G.G., H.L., M.C., and S.X. performed BSL-4 and ABSL-4 experiments. T.S. and Y.L. analyzed the data and wrote the initial manuscript. All authors approved the manuscript.

Competing interests

The authors declare no competing interests.

Additional information

Supplementary information The online version contains supplementary material available at https://doi.org/10.1038/s41541-025-01336-1.

Correspondence and requests for materials should be addressed to Chao Shan, Jingyi Liu or Hongjun Chen.